

RSC: Accelerating Graph Neural Networks Training via Randomized Sparse Computations

Zirui Liu
zl105@rice.edu
Rice University
United States

Shengyuan Chen
shengyuan.chen@connect.polyu.hk
Hong Kong Polytechnic University
Hong Kong

Kaixiong Zhou
kaixiong.zhou@rice.edu
Rice University
United States

Daochen Zha
daochen.zha@rice.edu
Rice University
United States

Xiao Huang
xiaohuang@comp.polyu.edu.hk
Hong Kong Polytechnic University
Hong Kong

Xia Hu
xia.hu@rice.edu
Rice University
United States

ABSTRACT

The training of graph neural networks (GNNs) is extremely time consuming because sparse graph-based operations are hard to be accelerated by hardware. Prior art explores trading off the computational precision to reduce the time complexity via sampling-based approximation. Based on the idea, previous works successfully accelerate the dense matrix based operations (e.g., convolution and linear) with negligible accuracy drop. However, unlike dense matrices, sparse matrices are stored in the irregular data format such that each row/column may have different number of non-zero entries. Thus, compared to the dense counterpart, approximating sparse operations has two unique challenges (1) we cannot directly control the efficiency of approximated sparse operation since the computation is only executed on non-zero entries; (2) sub-sampling sparse matrices is much more inefficient due to the irregular data format. To address the issues, our key idea is to control the accuracy-efficiency trade off by optimizing computation resource allocation layer-wisely and epoch-wisely. Specifically, for the **first** challenge, we customize the computation resource to different sparse operations, while limit the total used resource below a certain budget. For the **second** challenge, we cache previous sampled sparse matrices to reduce the epoch-wise sampling overhead. Finally, we propose a switching mechanisms to improve the generalization of GNNs trained with approximated operations. To this end, we propose **Randomized Sparse Computation**, which for the first time demonstrate the potential of training GNNs with approximated operations. In practice, RSC can achieve up to 11.6 \times speedup for a single sparse operation and a 1.6 \times end-to-end wall-clock time speedup with negligible accuracy drop.

CCS CONCEPTS

• **Computing methodologies** \rightarrow **Machine learning**.

KEYWORDS

Graph Neural Networks, Efficient Training, Randomized Algorithm

1 INTRODUCTION

Graph Neural Networks (GNNs) have achieved great success across different graph-related tasks [17, 21, 24, 36]. However, despite its effectiveness, the training of GNNs is very time consuming. Specifically, GNNs are characterized by an interleaved execution that

switches between the aggregation phase and the update phase. Namely, in the aggregation phase, every node aggregates messages from its neighborhoods at each layer, which is implemented based on sparse matrix-based operations. [15, 35] In the update phase, each node will update its embedding based on the aggregated messages, where the update function is implemented based on dense matrix-based operations [15, 35]. In Figure 1, SpMM and MatMul are the sparse operations and dense operations in the aggregation and update phase, respectively. Through profiling, we found that the aggregation phase may take more than 90% running time for GNN training. This is because the sparse matrix operations in the aggregation phase have many random memory accesses and limited data reuse, which is hard to be accelerated by community hardwares (e.g., CPUs and GPUs) [11, 12, 18]. Thus, training GNNs with large graphs is often time-inefficient.

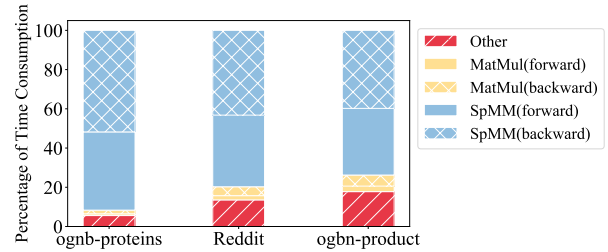


Figure 1: The time profiling of a two-layer GCNs on different datasets. SpMM may take 70% ~ 90% of the total training time.

Most of the existing works towards this problem can be roughly divided into three categories. First, some works propose the distributed GNNs training system with extra hardware [31, 34, 40]. Second, some works optimize the memory access pattern of sparse operations via coalescing the memory access and fusing consecutive operations [22, 30, 39]. Third, some works propose to accelerate the training process from the optimization aspect, i.e., using fewer iterations to converge [6, 29].

In parallel, another orthogonal direction is to replace the expensive operations with their faster approximated versions [1, 9]. The key idea is to sub-sample tensors onto low dimensional spaces and perform the original operations here. For example, for the linear operation between two matrices $A \in \mathbb{R}^{n \times m}$ and $B \in \mathbb{R}^{m \times q}$, we first obtain $A' \in \mathbb{R}^{n \times k}$ and $B' \in \mathbb{R}^{k \times q}$ ($k < m$) by selecting k representative columns of A and the corresponding rows of B based

on their euclidean norm [9]. Then we approximate $\mathbf{AB} \approx \mathbf{A}'\mathbf{B}'$. As a result, the number of floating-point operations (FLOPs) and memory access are both reduced. Based on the idea, previous work successfully accelerates the dense matrix based operations, such as convolution and linear operations [1]. The approximated operation can plug-and-play replace the exact operation to improve per-operation efficiency, and thus is compatible with most of the efficient training methods. Despite the potential, this perspective however has not been explored for the sparse operations in GNNs.

The approximation method reduces the computational complexity at the cost of giving noisy outputs, thus there naturally exists an **accuracy-efficiency trade off**. Compared to approximating dense matrix operations, it has two unique challenges to optimize the trade off for approximated sparse operations. First, unlike the previous example of approximating linear operation, k cannot directly control the efficiency (FLOPs) for sparse operations. This is because for dense matrices, each row/column has the same amount of parameters. Thus the reduction of FLOPs in approximated dense operations is totally decided by the dimensions of the sub-sampled matrices (i.e., k). However, in sparse operations, each row/column in the sparse adjacency matrix has different numbers of non-zero entries and the computation is only executed on non-zero entries (i.e., irregular data format). Thus, the reduction of FLOPs in the sparse operations is decided by the selection of representative row/columns. It lacks of the mechanism to directly control the efficiency-accuracy trade off for each sparse operation. Second, compared to the dense counterpart, slicing the sparse matrix is much more time-consuming due to this irregular data format [15], which counteracts the acceleration from the FLOPs reduction.

To this end, we propose **Randomized Sparse Computation**, dubbed RSC, the first approximation framework tailored for efficient GNN training. As we analyzed, unlike the dense counterpart, we lack the mechanism to directly control the efficiency-accuracy trade off for individual sparse operations. Instead, we propose to control the trade off by optimizing the computation resource allocation at the “global” level. Specifically, to tackle the first challenge, **at the layer-wise level**, since a GNN contains several sparse operations and each operation has a different importance to model accuracy, we propose to customize the FLOPs of different sparse operations while limiting the total FLOPs under a certain budget. Specifically, we frame it as a constraint optimization problem. Then we propose a greedy algorithm to efficiently solve it. To tackle the Second challenge, **at the epoch-wise level**, we found that the selection of representative row/columns tend to remain similar across nearby iterations. Based on this finding, we develop a caching mechanism to reuse the previous sampled sparse matrix across nearby iterations to reduce per-epoch sampling time. **Finally**, inspired by the recent finding that the final stage of training usually needs smaller noise to help convergence [26], we propose to use approximated sparse operation during most of the training process, while switch back to the original sparse operation at the final stage. We find that this switching mechanism significantly reduce the accuracy drop, at the cost of slightly less acceleration effect. In summary,

- We accelerate the training of GNNs from a brand new perspective, namely, replacing the expensive sparse operations with their faster approximated versions.

- Instead of focusing on balancing the efficiency-accuracy trade-off at operation level, we control the trade off through optimizing resource allocation at the layer-wise level and epoch-wise level.
- We propose a caching mechanism to reduce the per-epoch cost of sampling the sparse matrix by reusing previous results.
- We propose a switching mechanism to minimize the accuracy drop by switching back to the exact operations at the final stage.
- Extensive experiments have demonstrated the effectiveness of the proposed method. Particularly, RSC can achieve up to 11.6× speedup for a single sparse operation and a 1.6× end-to-end wall-clock time speedup with negligible ($\approx 0.3\%$) accuracy drop.

2 BACKGROUND AND PRELIMINARY

2.1 Graph Neural Networks

Let $\mathcal{G} = (\mathcal{V}, \mathcal{E})$ be an undirected graph with $\mathcal{V} = (v_1, \dots, v_{|\mathcal{V}|})$ and $\mathcal{E} = (e_1, \dots, e_{|\mathcal{E}|})$ being the set of nodes and edges, respectively. Let $\mathbf{X} \in \mathbb{R}^{|\mathcal{V}| \times d}$ be the node feature matrix. $\mathbf{A} \in \mathbb{R}^{|\mathcal{V}| \times |\mathcal{V}|}$ is the graph adjacency matrix, where $A_{i,j} = 1$ if $(v_i, v_j) \in \mathcal{E}$ else $A_{i,j} = 0$. $\tilde{\mathbf{A}} = \tilde{\mathbf{D}}^{-\frac{1}{2}}(\mathbf{A} + \mathbf{I})\tilde{\mathbf{D}}^{-\frac{1}{2}}$ is the normalized adjacency matrix, where $\tilde{\mathbf{D}}$ is the degree matrix of $\mathbf{A} + \mathbf{I}$. GNNs recursively update the embedding of a node by aggregating embeddings of its neighbors. For example, the forward pass of the l^{th} Graph Convolutional Network (GCN) layer [25] can be defined as:

$$\mathbf{H}^{(l+1)} = \text{ReLU}(\tilde{\mathbf{A}}\mathbf{H}^{(l)}\boldsymbol{\Theta}^{(l)}), \quad (1)$$

where $\mathbf{H}^{(l)}$ is the node embedding matrix at the l^{th} layer and $\mathbf{H}^{(0)} = \mathbf{X}$. $\boldsymbol{\Theta}^{(l)}$ is the weight matrix of the l^{th} GCN layer.

In practice, $\tilde{\mathbf{A}}$ is often stored in the sparse matrix format, e.g., compressed sparse row (CSR) [15]. From the implementation aspect, the computation of Equation (1) can be described as:

$$\mathbf{H}^{(l+1)} = \text{ReLU}\left(\text{SpMM}\left(\tilde{\mathbf{A}}, \text{MatMul}(\mathbf{H}^{(l)}, \boldsymbol{\Theta}^{(l)})\right)\right), \quad (2)$$

where $\text{SpMM}(\cdot, \cdot)$ is the Sparse-Dense Matrix Multiplication and $\text{MatMul}(\cdot, \cdot)$ is the Dense Matrix Multiplication. Unlike dense matrices, the elements are randomly distributed in the sparse matrix. Thus sparse operations, such as SpMM, have many random memory accesses and are much slower than the dense counterpart [11, 18]. To get a sense of the scale, we shown in Figure 1 that for GCNs, SpMM may take roughly 70% ~ 90% of the total training time.

2.2 Fast Approximated MatMul with Sampling

Let $\mathbf{X} \in \mathbb{R}^{n \times m}$, $\mathbf{Y} \in \mathbb{R}^{m \times q}$. The goal is to efficiently estimate the matrix production \mathbf{XY} . Truncated Singular Value Decomposition (SVD) outputs provably optimal low-rank estimation of \mathbf{XY} [1]. However, SVD is almost as expensive as the matrix production itself. Instead, the sampling algorithm is proposed to approximate the matrix product \mathbf{XY} by sampling k columns of \mathbf{X} and corresponding rows of \mathbf{Y} to form smaller matrices, which are then multiplied as usual [9]. This algorithm reduces the computational complexity from $O(mnq)$ to $O(knq)$. Specifically,

$$\begin{aligned} \mathbf{XY} &= \sum_{i=1}^m \mathbf{X}_{:,i} \mathbf{Y}_{i,:} \approx \sum_{t=1}^k \frac{1}{s_t} \mathbf{X}_{:,i_t} \mathbf{Y}_{i_t,:} \\ &= \text{approx}(\mathbf{XY}), \end{aligned} \quad (3)$$

where $X_{:,i} \in \mathbb{R}^{n \times 1}$ and $Y_{i,:} \in \mathbb{R}^{1 \times q}$ are the i^{th} column and row of X and Y , respectively. In this paper, we call $(X_{:,i}, Y_{i,:})$ the i^{th} column-row pair. k is the number of samples ($1 \leq k \leq m$). $\{p_i\}_{i=1}^m$ is a probability distribution over the column-row pairs. $i_t \in \{1, \dots, m\}$ is the index of the sampled column-row pair at the t^{th} trial. s_t is the scale factor. Theoretically, [9] shows that if we set $s_t = \frac{1}{kp_{i_t}}$, then we have $\mathbb{E}[\text{approx}(XY)] = XY$. Further, the expectation of approximation error $\mathbb{E}[\|XY - \text{approx}(XY)\|_F]$ is minimized when the sampling probabilities $\{p_i\}_{i=1}^m$ are proportional to the product of the column-row Euclidean norms [9]:

$$p_i = \frac{\|X_{:,i}\|_2 \|Y_{i,:}\|_2}{\sum_{j=1}^m \|X_{:,j}\|_2 \|Y_{j,:}\|_2}. \quad (4)$$

2.2.1 Top- k sampling. The above sampling based approximation method is originally developed for accelerating the general application of dense matrix multiplication [9]. Directly applying it to neural network may be sub-optimal because it does not consider the characteristic of neural networks. [1] modifies the sampling algorithm by taking the weight distribution of neural network into account. Based on the empirical observation that the distribution of weights remains centered around zero during training [16, 19], [1] proposes a top- k sampling algorithm as follows:

top- k sampling: Selecting k column-row pairs with the largest $\frac{\|X_{:,i}\|_2 \|Y_{i,:}\|_2}{\sum_{j=1}^m \|X_{:,j}\|_2 \|Y_{j,:}\|_2}$ values deterministically without scaling.

Equivalently, it means p_i of column-row pairs with the k -largest value in Equation (4) equals 1, otherwise it equals 0. And s_{i_t} is a constant 1. Albeit without the scaling while sampling column-row pairs deterministically, under on the assumption of zero-centered weight distribution, [1] theoretically show that *top- k sampling still yield an unbiased estimation of AB with minimal approximation error*. Consequently, the top- k sampling algorithm empirically shows significantly lower accuracy drop when approximating the convolution and linear operations in the neural networks [1].

Note that the approximation method reduces not only FLOPs, but also the number of memory accesses since we do not need to read the dropped elements, which is crucial for accelerating memory-bound operation, such as SpMM [18].

In the next section, we explore how to approximate the expensive sparse operation via the top- k sampling.

3 THE PROPOSED FRAMEWORK

The overview of our proposed framework is shown in Figure 2, where we use the computation graph of GCN as an example. We first explore which SpMM in the computation graph can be replaced with its approximated version (Section 3.1). Then since GNNs have multiple SpMM and each of them may have different importance to the model performance, we then automatically allocate computation resource to different SpMM (Section 3.2). Finally, we explore two simple and effective tricks for improving RSC. The first one is the caching mechanism to reduce the overhead of sampling sparse matrices (Section 3.3.1), the second one is the switching mechanism to reduce the accuracy drop (Section 3.3.2).

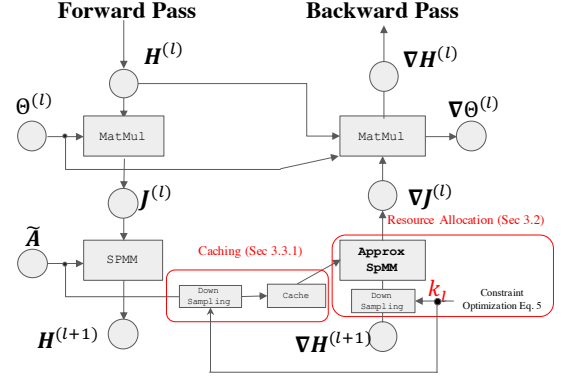


Figure 2: Overview of RSC. For convenience, ReLU is ignored. RSC only replace the SpMM in the backward pass with its approximated version using top- k sampling (Section 3.1). k_l is the number of samples for top- k sampling at the l^{th} layer, which is automatically allocated (Section 3.2). To reduce the overhead of sampling, we also cache the sampled graph and reuse it across nearby iterations (Section 3.3).

3.1 Where to Apply the Approximation

3.1.1 Experimental analysis. Each sparse operation is executed twice at each training step, i.e., one in the forward pass and the other one in the backward pass. As shown in Figure 2, here we take SpMM in the l^{th} GCN layer as an example, the forward one is $H^{(l+1)} = \text{ReLU}(\text{SpMM}(\tilde{A}, J^{(l)}))$, where $J^{(l)} = \text{MatMul}(H^{(l)}, \Theta^{(l)})$ is the intermediate node representations. And the backward one is $\nabla J^{(l)} = \text{SpMM}(\tilde{A}^T, \nabla H^{(l+1)})$. $\nabla J^{(l)}$ and $\nabla H^{(l)}$ are the gradient with respect to $J^{(l)}$ and $H^{(l)}$, respectively.

Even though the approximation method itself is statistically unbiased, replacing the exact sparse operation with their faster approximated versions still injects noise to the computation graph, and the noise will be propagated layer-by-layer during the training. As we analyzed above, each SpMM is executed twice in the training step. Below we first experimentally analyze the impact of the injected noise in the forward pass and the backward pass. As shown in Table 1, we apply top- k sampling to approximate the SpMM in the forward pass, backward pass, or both, respectively.

Table 1: Preliminary results on approximating SpMM via top- k sampling. The model is a two-layer GCN and dataset is Reddit. Here we set the k as $0.1|V|$ across different layers.

Method	Reddit
without approximation	95.39±0.04
only forward	16.45±0.39
only backward	95.25±0.03
forward and backward	80.74±1.00

From Table 1, the accuracy drop is negligible if we only replace SpMM in the backward pass. Notably, if we apply approximation in both the forward and backward pass, the result is significantly better than only applying top- k sampling in the forward pass. The reason is that when only applying approximation in the forward pass, some row/columns are not included in the computation graph, so

intuitively these row/columns should be excluded in the backward pass. “forward and backward” result in Table 1 is built based on this intuition such that in the backward pass, we use the column-row pairs sampled in the forward pass to compute the gradient. However, it is still not comparable to the result of applying approximation only in the backward pass. Below we mathematically analyze the reason behind the results in Table 1.

3.1.2 Theoretical analysis. We first analyze the case of approximating the sparse operations in the forward pass. Namely, replacing $\text{SpMM}(\tilde{\mathbf{A}}, \mathbf{J}^{(l)})$ with $\text{approx}(\tilde{\mathbf{A}}\mathbf{J}^{(l)})$. We note that we have $\mathbb{E}[f(x)] \neq f(\mathbb{E}[x])$ for any non-linear function $f(\cdot)$, e.g., $\mathbb{E}[x^2] \neq \mathbb{E}^2[x]$. Thus, even when the approximation method gives an unbiased estimation, i.e., $\mathbb{E}[\text{approx}(\tilde{\mathbf{A}}\mathbf{J}^{(l)})] = \tilde{\mathbf{A}}\mathbf{J}^{(l)}$, the node embeddings $\mathbf{H}^{(l+1)}$ are still biased since the activation function is non-linear. To see this,

$$\begin{aligned}\mathbb{E}[\mathbf{H}^{(l+1)}] &= \mathbb{E}[\text{ReLU}(\text{approx}(\tilde{\mathbf{A}}\mathbf{J}^{(l)}))] \\ &\neq \text{ReLU}(\mathbb{E}[\text{approx}(\tilde{\mathbf{A}}\mathbf{J}^{(l)})]) = \mathbf{H}^{(l+1)}.\end{aligned}$$

Thus, if we apply the approximation for the SpMM in the forward pass, the bias will be propagated layer-by-layer and cause significantly worse results. For the case of only approximating the sparse operation in the backward pass, we have the following proposition:

Proposition 1 (Proof in Appendix A). *If the approximation method is itself unbiased, and we only replace the SpMM in the backward pass with its approximated version, while leaving the forward one unchanged, then the calculated gradient is provably unbiased.*

Due to the page limit, the proof is deferred to the Appendix. The high level idea is that the gradient of activation function in backward pass is only related to the pre-activations in the forward pass, and thus is independent to the approximation error introduced in the backward pass. As suggested by our theoretical and empirical analysis, as shown in Figure 2, **we only approximate the sparse operations in the backward pass, while leaving all other operations unchanged.** Namely, we replace the exact sparse operation $\nabla \mathbf{J}^{(l)} = \text{SpMM}(\tilde{\mathbf{A}}^\top, \nabla \mathbf{H}^{(l+1)})$ in the backward pass with $\text{approx}(\tilde{\mathbf{A}}^\top \nabla \mathbf{H}^{(l+1)})$ using top- k sampling.

3.2 How to Apply the Approximation

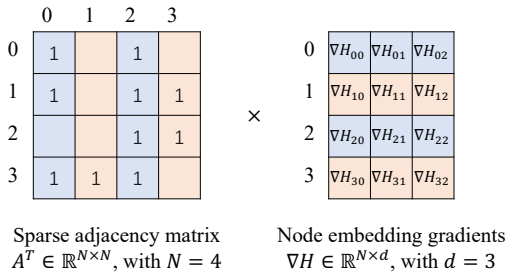


Figure 3: For approximated sparse operations, the acceleration is decided by the selection of column-row pairs. For example, selecting orange column-row pairs entails $\frac{3}{7} \times$ less FLOPs and memory access compared to the blue pairs, since these orange low-degree nodes associate with less non-zero entries in the adjacency matrix.

In the last section, we explored where to place the approximation method. However, as we mentioned in the introduction, for sparse operations, the acceleration is decided by the selection of sampled column-row pairs. To see this, as shown in Figure 3, suppose we use top- k sampling to approximate $\text{SpMM}(\tilde{\mathbf{A}}^\top, \nabla \mathbf{H})$. Since the computations are only executed on the non-zero entries, so selecting the orange pairs (i.e., pair 1 and 3) will result in $\frac{3}{7} \times$ less computational cost (FLOPs) compared to selecting the blue pair (i.e., pair 0 and 2). For both the orange and blue cases, we have $k = 2$. Thus, the number of samples k cannot directly constrain the FLOPs for each individual operation. Moreover, a GNN has multiple layers (or operations) and each layer has a different importance to the model accuracy. To optimize the accuracy-efficiency trade off, our key idea is to customize the computation resources (i.e., FLOPs) for each layer by adjusting the number of samples k_l in the l -th layer. In this way, we minimize the impact of approximation, while limiting the overall FLOPs under a certain budget. Based on the idea, we frame the resource allocation problem as the following constrained optimization problem:

$$\min_{\{k_l\}} - \sum_{l=1}^L \sum_{i \in \text{Top}_{k_l}} \|\tilde{\mathbf{A}}_{:,i}^\top\|_2 \|\nabla \mathbf{H}_{i,:}^{(l+1)}\|_2, \quad (5a)$$

$$\text{s.t.} \sum_{l=1}^L \sum_{i \in \text{Top}_{k_l}} \#nnz_i * d_l \leq C \sum_{i=1}^L |\mathcal{E}| d_l, \quad (5b)$$

where C is the budget ($0 < C < 1$) that controls the overall reduced FLOPs. k_l is the number of samples for the top- k sampling at the l -th layer. d_l is the hidden dimensions of l -th layer, and $\#nnz_i$ is the number of non-zero entries at the i -th column of $\tilde{\mathbf{A}}^\top$. Top_{k_l} is the set of indices associated with the k_l largest $\|\tilde{\mathbf{A}}_{:,i}^\top\|_2 \|\nabla \mathbf{H}_{i,:}^{(l+1)}\|_2$.

Equation (5a) is equivalent to minimizing approximation error $\mathbb{E}[\|\tilde{\mathbf{A}}^\top \nabla \mathbf{H}^{(l+1)} - \text{approx}(\tilde{\mathbf{A}}^\top \nabla \mathbf{H}^{(l+1)})\|_F]$ summarized over all layers [1]. Also, different sparse operations are weighted summation by the magnitude of gradient $\|\nabla \mathbf{H}^{(l+1)}\|_2$, which implicitly encodes the importance of different operations.

Equation (5b) is the constraint that controls the overall FLOPs. Specifically, the FLOPs of SpMM between $\tilde{\mathbf{A}}$ and the gradient $\nabla \mathbf{H} \in \mathbb{R}^{N \times d}$ is $\mathcal{O}(|\mathcal{E}|d)$ and $\sum_{j \in \mathcal{V}} \#nnz_j = |\mathcal{E}|$. Since for sparse operations, the reduction in the number of memory access and FLOPs are linearly correlated, Equation (5b) also bounds the number of memory access.

3.2.1 Greedy solution. The above combination optimization objective is NP-hard, albeit it can be solved by dynamic programming. However, the dynamic programming is very slow, which somehow contradicts with our purpose of being efficient. Thus, we propose to use a greedy algorithm to solve it. Specifically, it starts with highest $k_l = |\mathcal{V}|$ for all layers. In each move, it chooses a k_l among $\{k_l\}_{l=1}^L$ to reduce by a step size (e.g., $0.02|\mathcal{V}|$), such that the increment of errors in Equation (5a) is minimal. The greedy algorithm will stop when the current total FLOPs fits in the budget in Equation (5b). This algorithm runs super fast and we found that it has minimal impact to the efficiency. We provide the pseudo code of our greedy algorithm in Algorithm 1 of Appendix B.

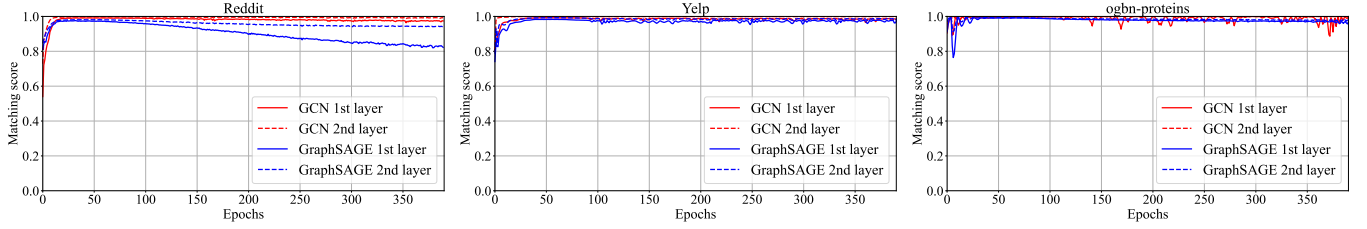


Figure 4: For each layer, the selected column-row pairs tend to be very similar across iterations. Models here are two-layer GCN and GraphSAGE. Here we show the matching scores (AUC) of top- k indices between every 10 steps.

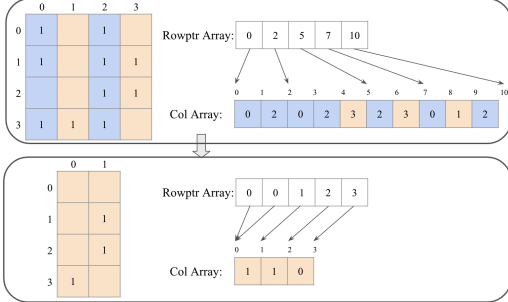


Figure 5: The process of slicing the sparse matrix in Figure 3 by only reserving orange columns (in CSR format), which requires to re-build the Rowptr and Col Array.

3.3 When to Apply the Approximation

3.3.1 Cache the sampled sparse matrices. Before illustrating the caching mechanism, we first give the details about the Compressed Sparse Row (CSR) format for representing the sparse matrix here. CSR stores nonzero values in a matrix and their position in three arrays: index array Rowptr, column array Col, and value array Val. The elements in Rowptr act as the starting indices of the elements in Col and Val that correspond to each row. Specifically, the elements of row i are stored in indices Rowptr[i] to Rowptr[$i+1$] - 1 of Col and Val. The elements in Col and Val are the column index and value in that column, respectively. Figure 5 shows the CSR format of the matrix shown in Figure 3. We ignore the Val array here since the sparse matrix contains only element one.

As shown in Figure 2, RSC reduces the number of FLOPs and memory access via top- k sampling. From the implementation aspect, executing the top- k sampling contains two steps: First, it decides the indices corresponding to the top- k largest column row norms in Equation (4). Second, slicing the matrices according to the indices. In practice, the overhead of calculating the column-row norms can be ignored. However, unlike dense matrices, slicing the adjacency matrix is very slow due to its irregular data format. To see this, suppose the top- k indices of the sparse matrix in Figure 3 correspond to the orange column-row pairs. We show in Figure 5 the process of slicing the adjacency matrix in CSR format by reserving only the orange columns [15]. Compared to slicing dense matrices, slicing sparse matrices requires to re-process the graph to build the new Rowptr and Col, which introduces significant time overhead, especially for large graphs.

For the full graph training, we use the same adjacency matrix across different epochs¹. We made a crucial observation that the

¹For sub-graph based training, we can first sample all of the sub-graphs offline. Then during the training, we apply the caching mechanism to each sampled graph.

top- k indices in the adjacency matrix tend to be the same across iterations. In Figure 4, we plot the AUC score of top- k indices between every iteration t and iteration $t + 10$ for each layer throughout the whole training process. Here we note that AUC score is a commonly used ranking measure and a 1.0 AUC score means the ranking of column-row pairs is identical across iterations. The results in Figure 4 indicate that the top- k indices won't change significantly within a few iterations. Thus, as shown in Figure 2, we propose to reuse the sampled adjacency matrix for each layer across nearby iterations for reducing the overhead. In Section 5, we experimentally show that the caching mechanism does not impact the model performance a lot, but leading to significant speedup.

3.3.2 Switch back to origin sparse operation at the end. When training neural networks, the common practice is to use a large learning rate for exploration and anneal to a small one for final convergence [26]. The rationale behind this strategy is that, at the end of the training process, we need to fine-tune our model with small noise for convergence. Since our approximation sparse operations will bring extra noise to the gradient, intuitively, we can switch back to the original sparse operations to help convergence. More formally, we propose to use approximated sparse operation during most of the training process, while switching back to the original sparse operation at the final stage. We experimentally show that this switching mechanism significantly reduces the accuracy drop, at the cost of slightly less acceleration effect.

3.4 Connections to Graph Data Augmentation

Data augmentation [20, 27] is widely adopted in the graph learning for improving model generalization, including dropping nodes [14], dropping edges [32], and graph mixup [20]. As shown in Figure 5, the top- k sampling drops the entire columns in the adjacency matrix, while keeping the number of rows unchanged. **That means RSC drops all of the out edges for a set of nodes.** This can be viewed as the "structural droppedge" for improving the efficiency. Since we only apply the top- k sampling in the backward pass and top- k indices are different for each operation, **RSC essentially forward pass with the whole graph, backward pass with different subgraphs at each layer.** This structural droppedge and heterogeneous backward propagation introduce the regularization effect. Thus as shown in the experiment section, RSC may also improve the model accuracy over the baseline.

4 RELATED WORK AND DISCUSSION

In this section, we first discuss the related work. Then we discuss the limitations of our work.

Subgraph-based GNN training. The key idea of this line of work is to improve the scalability of GNNs by separating the graph into overlapped small batches, then training models with sampled subgraphs [4, 17, 23, 38, 41]. However, this approach reduces the memory footprint but results in extra time cost to compute the overlapping nodes between batches. Generally, methods in this category are orthogonal to RSC, and they can be combined, which is shown in the next section.

Approximated Matrix Multiplication. The known algorithms for approximating matrix production can be roughly divided into three categories. However, only a few of them can be used for accelerating GNN training.

- Random walk-based methods [5] performs random walks on a graph representation of the dense matrices, but is applicable to non-negative matrices only.
- Butterfly-based methods [2, 7] replace dense matrices with butterfly matrices. It is not applicable to SpMM in GNNs because the adjacency matrix often cannot be reduced to a butterfly matrix.
- Column-row sampling methods [8, 10] subsample the input matrices with important rows and columns, then perform the production on sampled matrix as usual.

Other randomized GNN training. Dropedge [32] randomly drops edges to avoid the over-smoothing problem. Graph Random Neural Networks (Grand) [14] randomly drop nodes to generate data augmentation for improving model generalization. Grand+ improves the scalability over Grand by **pre-computing** a general propagation matrix and employ it to perform data augmentation [13]. As shown in Section 3.4, the key difference between GRAND(+) and RSC is that **RSC does not drop any node. Instead RSC drops all of the out edges for a set of nodes only during backward pass. Moreover, the drop pattern are evolving during the training process.** This can be viewed as the “structural dropedge”. However, unlike Dropedge [32], RSC drop the column-row pairs according to the euclidean norm instead of uniformly dropping.

Limitations of RSC. First, to guarantee the model accuracy, we only replace the sparse operation in the backward pass. Thus the upper bound of RSC’s speedup is limited. However, we note that the backward pass usually is more time-consuming than the forward pass, which is also empirically shown in Table 2. Second, some GNNs rely on the scatter-and-gather instead of SpMM (and its variant) to perform the aggregation, such as GAT [33]. They are not covered in this paper. However, scatter-and-gather based GNNs can also be accelerated by RSC because the column-row sampling is also applicable to scatter and gather operation. Similarly, the caching and switching mechanisms are also applicable to them. However, for the resource allocation Algorithm 1, the scatter and gather operations requires tailored error bound and the computation cost modeling in Equation (5). We leave it as the future work.

5 EXPERIMENTS

We verify the effectiveness of our proposed framework through answering the following research questions:

- **Q1:** How effective is RSC in terms of the accuracy with reduced training time?

- **Q2:** How effective is our proposed allocation strategy compared to the uniform allocation strategy?
- **Q3:** What is the layer-wise ratio assigned by RSC?
- **Q4:** How effective is the caching and switching mechanism in terms of the trade-off between efficiency and accuracy?
- **Q5:** How sensitive is RSC to its key hyperparameters?

5.1 Experimental Settings

Datasets and Baselines. To evaluate RSC, we adopt four common large scale graph benchmarks from different domains, i.e., Reddit [17], Yelp [38], *ogbn-proteins* [21], and *ogbn-products* [21]. We evaluate RSC under both the mini-batch training and full-batch training settings. For the mini-batch training setting, we integrate RSC with one of the state-of-the-art sampling methods, GraphSAINT [38]. For the full-batch training setting, we integrate RSC with three popular models: two commonly used shallow models, namely, GCN [25] and GraphSAGE [17], and one deep model GCNII [3]. To avoid creating confusion, GCN, GraphSAGE, and GCNII are all trained with the whole graph at each step. For a fair comparison, we use the MEAN aggregator for GraphSAGE and GraphSAINT throughout the paper. Details about the hyperparameters and datasets are in Appendix C.

Hyperparameter settings. RSC contains three parts. First, the allocation strategy. We choose the overall budget C in Equation (5b) from $\{0.1, 0.3, 0.5\}$. We run the resource allocation strategy every **ten** steps. The step size α in Algorithm 1 is set as $0.02/|\mathcal{V}|$. Second, the caching mechanism. According to Figure 4, we sample the adjacency matrix every **10** steps and reuse the sampled sparse matrix for nearby steps. Third, the switching mechanism, where we apply RSC for **80%** of the total epochs, while switching back to the original operations for the rest of the **20%** epochs.

Evaluation metrics. To evaluate the practical usage of RSC, we report the wall clock time speedup measured on GPUs. Specifically, the speedup equals $T_{\text{baseline}}/T_{\text{rsc}}$, where T_{baseline} and T_{rsc} are the wall clock training time of baseline and RSC, respectively. We note that the T_{rsc} includes the running time of the greedy algorithm in Section 3.2.1, as well as the effects of caching and switching.

5.2 Performance Analysis

5.2.1 Accuracy-efficiency trade-off. To answer **Q1**, we summarize the speedup and the test accuracy/F1-micro/AUC of different methods in Table 3. Since RSC accelerates the sparse operation in the backward pass, we also provide the detailed efficiency analysis in Table 2. In summary, we observe:

① *At the operation level, RSC can accelerate the sparse operation in the backward pass by up to 11.6×. For end-to-end training, the accuracy drop of applying RSC over baselines is negligible (0.3%) across different models and datasets, while achieving up to 1.6× end-to-end wall clock time speedup.* The gap between the operation speedup and the end-to-end speedup are due to the following two reasons. First, we focus on accelerating the sparse computations in GNNs, which is the unique bottleneck to GNNs. The other dense computations can certainly be accelerated by approximation methods, but this beyond the scope of this paper. Second, according to our theoretical analysis, we only accelerate the sparse computation in the backward pass instead of the forward one to guarantee the performance. **We note**

Table 2: Comparison on the efficiency at the operation level. fwd is the wall-clock time for a single forward pass (ms), bwd is the wall-clock time for a single backward pass (ms). SpMM_MEAN is one variant of SpMM, which corresponds to the MEAN aggregator used in GraphSAGE (Appendix A.2). RSC can reduce the wall clock time of backward sparse computation by up to 11.6 \times .

		Reddit		Yelp		ogbn-proteins		ogbn-products	
		fwd	bwd	fwd	bwd	fwd	bwd	fwd	bwd
SpMM	Baseline	36.28	44.23	26.88	34.38	31.72	42.99	261.03	316.80
	+RSC	-	3.81 (11.6 \times)	-	9.86 (3.49 \times)	-	14.87 (2.89 \times)	-	35.28 (8.98 \times)
SpMM_MEAN (Appendix A.2)	Baseline	36.21	44.27	26.78	34.38	31.80	43.11	261.03	316.84
	+RSC	-	7.47 (5.92 \times)	-	19.62 (1.75 \times)	-	5.22 (8.26 \times)	-	71.59 (4.43 \times)

Table 3: Comparison on the test accuracy/F1-micro/AUC and speedup on four datasets. Bold faces indicate the accuracy drop is negligible ($\approx 0.3\%$) or the result is better compared to the baseline. The hardware here is a RTX3090 (24GB). All reported results are averaged over ten random trials.

	# nodes	230K			717K			132K			2.4M		
	# edges	11.6M			7.9M			39.5M			61.9M		
Model	Methods	Reddit			Yelp			ogbn-proteins			ogbn-products		
		Acc.	Budget C	Speedup	F1-micro	Budget C	Speedup	AUC	Budget C	Speedup	Acc.	Budget C	Speedup
GraphSAINT	Baseline	96.40±0.03	1	1×	63.30±0.14	1	1×	—	—	—	79.01±0.21	1	1×
	+RSC	96.24±0.03	0.1	1.11×	63.34±0.18	0.1	1.09×	—	—	—	78.99±0.32	0.3	1.04×
GCN	Baseline	95.33±0.03	1	1×	44.28±1.04	1	1×	71.99±0.66	1	1×	75.74±0.11	1	1×
	+RSC	95.13±0.05	0.1	1.47×	46.09±0.54	0.1	1.17×	71.60±0.45	0.3	1.51×	75.44±0.21	0.3	1.35×
GraphSAGE (full batch)	Baseline	96.61±0.05	1	1×	63.06±0.18	1	1×	76.09±0.77	1	1×	78.73 ± 0.12	1	1×
	+RSC	96.52±0.04	0.1	1.32×	62.89±0.19	0.1	1.13×	76.30±0.42	0.3	1.60×	78.50± 0.09	0.1	1.53×
GCNII	Baseline	96.71±0.07	1	1×	63.45±0.17	1	1×	73.79±1.32	1	1×	—	—	—
	+RSC	96.50±0.12	0.3	1.45×	63.57±0.21	0.1	1.19×	75.20±0.54	0.5	1.41×	—	—	—

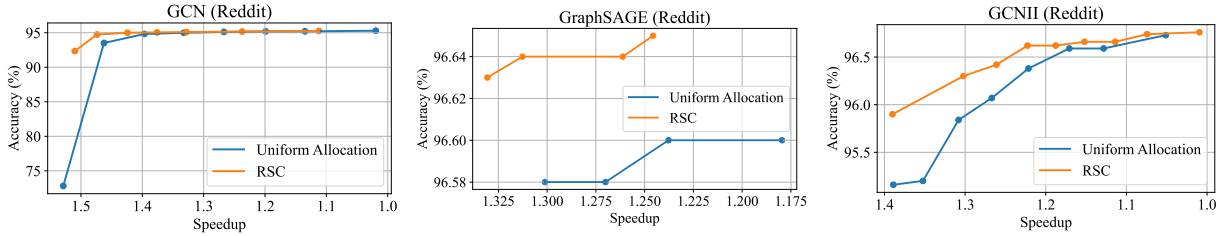


Figure 6: The Pareto frontier of the accuracy-efficiency trade-off for RSC and the uniform allocation. Here we disabled the caching and switch mechanism for a fair comparison. All results are averaged over five random trials.

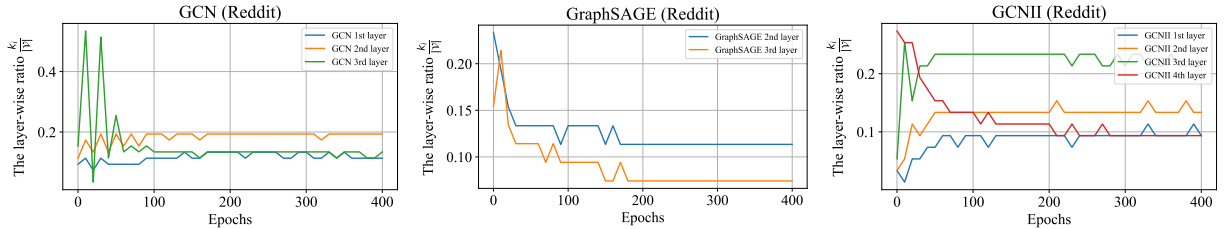


Figure 7: The allocated layer-wise k_l for GCN, GraphSAGE and GCNII on Reddit, where the overall budget C is set as 0.1. The input of the SpMM in the first GraphSAGE layer does not require gradient and thus absent in the Figure (Appendix A.2).

that for approximation methods that accelerate the training process at operation level, a $1.2 \approx 1.3\times$ wall-clock speedup with negligible accuracy drop can be regarded as non-trivial (for details, please see Table 1 in [1]), especially considering that these approximation methods are orthogonal to most of the existing efficient training methods. For GraphSAINT, the speedup of RSC is around $1.1\times$, which is smaller than the full graph training. This

is because for subgraph-based training, the equivalent “batch size” is much smaller than the full graph counterparts. As a result, the GPU utility is low since it does not assign each processor sufficient amount of work [37]. The speedup for subgraph training is expected to improve when using larger batch size.

② *The proper hyperparameter C varies with datasets and models.* As shown in Table 3, the overall budget C varies across dataset and

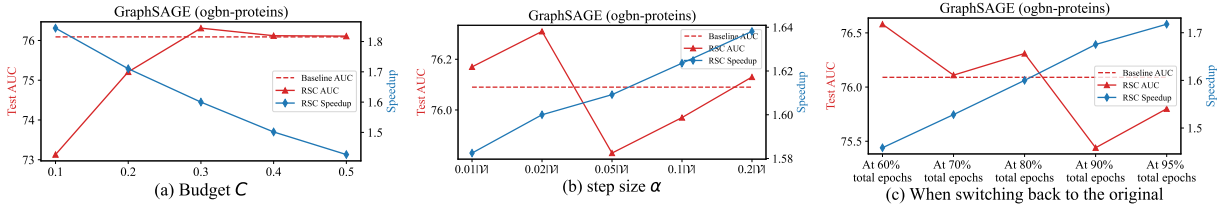


Figure 8: Hyperparameter analysis w.r.t. the budget C , the step size α in Algorithm 1, and when switching back to the original operations. The model is GraphSAGE and the applied dataset is ogbn-proteins.

models. For example, for ogbn-proteins, the overall budget C is 0.3 for GCN and GraphSAGE, while it is 0.5 for GCNII. For Reddit, the overall budget C is 0.1 for GCN and GraphSAGE, while it is 0.3 for GCNII. In general, deep GNNs may require a larger C compared to the shallow GNNs. This is because deeper GNNs are more sensitive to the approximation errors due to the fact that the approximation error will compound layer-by-layer during the backward pass [28].

5.2.2 The role of resource allocation strategy. Each sparse operation has a different importance to the model accuracy. Thus when allocating the same k_l to different sparse operations, it may either harm the model performance with insufficient k_l or waste resources on unimportant operations. To answer Q2, we compare RSC with the uniform allocation strategy, i.e., setting $k_l = C|V|$ for all sparse operations in the backward pass. As shown in Figure 6, we plot the Pareto frontier of the accuracy-efficiency trade-off on Reddit dataset for RSC and the uniform strategy with different C . For a fair comparison, we disabled the caching and switching mechanism. Due to the page limit, we show the running time of the greedy algorithm in Table 5 of Appendix B. We conclude that the overhead of greedy algorithm is negligible compared to the acceleration effect of RSC. In summary, we observe that:

③ RSC exhibits a superior trade-off between accuracy and efficiency compared to the uniform allocation, especially under high speedup regime. Namely, compared to the uniform allocation, RSC can achieve higher model accuracy under the same speedup. This can be explained by the fact that each operation has a different importance to the model performance. RSC can automatically allocate more resource to important operations under a given total budget.

To answer Q3, we also visualize the allocated k_l for each layer across iterations in Figure 7 (as mentioned in Section 5.1, the resource allocation algorithm is executed every ten steps). We note that the input of the SpMM in the first GraphSAGE layer does not require gradient and thus does not appear in Figure 7, which we will elaborate more details in Appendix A.2.

④ The k_l assigned by RSC evolves along with the training process. From Figure 7, the allocated k_l changes rapidly in the initial phase and starts to converge at about 100th epochs. Due to the page limit, we also visualize the degree of picked nodes in Figure 9 in the Appendix. We conclude that the preference of different layers also evolves during the training process.

5.2.3 The role of caching and switching mechanism. In section 5.2.2, we have shown the superior results of the proposed resource allocation strategy. As we mentioned in Section 3.3, we also introduce two simple tricks to for improving RSC, i.e., the caching and switching mechanism. To verify the effect of each of them (Q4), we conduct

Table 4: Ablation on the caching and switching mechanism. Experiments are conducted on ogbn-proteins. All results are averaged over five random trials.

Ablation on	Caching	Switching	AUC	Speedup
GCN	✗	✗	71.60 ± 0.66	1.19×
	✗	✓	72.19 ± 0.79	1.14×
	✓	✗	69.80 ± 0.60	1.60×
	✓	✓	71.60 ± 0.45	1.51×
GraphSAGE	✗	✗	75.23 ± 0.79	1.37×
	✗	✓	76.39 ± 0.39	1.32×
	✓	✗	75.53 ± 0.60	1.78×
	✓	✓	76.30 ± 0.42	1.60×
GCNII	✗	✗	74.07 ± 0.83	1.10×
	✗	✓	74.50 ± 0.52	1.04×
	✓	✗	72.47 ± 0.75	1.46×
	✓	✓	75.20 ± 0.54	1.41×

incremental evaluations on GCN, GraphSAGE and GCNII with ogbn-proteins, which are summarized in Table 4. The row without caching and switching in Table 4 corresponds to the results with proposed resource allocation strategy. We observe that:

⑤ Switching mechanism significantly improves the model performance, at the cost of slightly less acceleration effect. Specifically, compared to the results with only resource allocation strategy, the switching mechanism improves 0.59%, 1.16%, and 0.43% AUC, at the cost of 0.05×, 0.05×, and 0.06× less speedup for GCN, GraphSAGE, and GCNII, respectively. As we analyzed in Section 3.3.2, the improvement can be explained by the fact that the final training stage requires smaller gradient noise to help convergence.

⑥ Caching mechanism significantly improves the wall-clock time speedup, at the cost of worse model performance. Specifically, compared to the results with only resource allocation strategy, the caching mechanism improves 34.4%, 29.9%, and 32.7% speedup, at the cost of 1.8%, -0.3%, and 1.6% less AUC for GCN, GraphSAGE, and GCNII, respectively. Although caching mechanism can significantly reduce the overhead of sampling, the performance drop is too large (> 1%). Intuitively, the accuracy drop of caching also implies that we could not use a “static” down-sampled graph throughout the training process.

⑦ Surprisingly, jointly applying the caching and switching, the performance drop can be minimized. Specifically, compared to the results with only resource allocation strategy, when jointly applying the caching and switching, it improves 0.0%, 1.07%, and 1.13% model performance, while achieving 0.22×, 0.23×, and 0.2× more speedup simultaneously. In summary, jointly applying the caching and switching enables a “win-win” in terms of the model performance and training efficiency.

5.2.4 Hyperparameter sensitivity analysis (Q5). Here we analyze the impacts of the main hyperparameters of RSC : (1) the budget C , which controls the efficiency-accuracy trade off; (2) the step size α in the greedy Algorithm 1; (3) when switching back to the original sparse operations. In Figure 8, we vary only one of them with the others fixed. We conclude (1) larger budget C leads to better accuracy with smaller speedup, since we are using more computational resources to approximate the full operation. (2) larger step size α leads to marginally larger speedup since the greedy algorithm will terminate earlier. Also the step size α does not affect the model accuracy a lot. In practice, we set $\alpha = 0.02|\mathcal{V}|$. (3) The later we switch back to the original operation, the larger the accuracy drop and the smaller the speedup, it is equivalent to using less resources to approximate the full operation epoch-wisely. Thus, we apply RSC for 80% of the total epochs to balance the trade-off.

6 CONCLUSIONS AND FUTURE WORK

In this paper, we propose RSC, which replaces the sparse computations in GNNs with their fast approximated versions. RSC can be plugged into most of the existing training frameworks to improve their efficiency. Future work includes (1) exploring other types of approximation methods. (2) exploring RSC for GNNs that relies on scatter-and-gather operations.

REFERENCES

- [1] Menachem Adelman, Kfir Levy, Ido Hakimi, and Mark Silberstein. 2021. Faster neural network training with approximate tensor operations. *Advances in Neural Information Processing Systems* 34 (2021), 27877–27889.
- [2] Beidi Chen, Tri Dao, Kaizhao Liang, Jiaming Yang, Zhao Song, Atri Rudra, and Christopher Re. 2021. Pixelated butterfly: Simple and efficient sparse training for neural network models. *arXiv preprint arXiv:2112.00029* (2021).
- [3] Ming Chen, Zhewei Wei, Zengfeng Huang, Bolin Ding, and Yaliang Li. 2020. Simple and deep graph convolutional networks. In *International Conference on Machine Learning*. PMLR, 1725–1735.
- [4] Wei-Lin Chiang, Xuanqing Liu, Si Si, Yang Li, Samy Bengio, and Cho-Jui Hsieh. 2019. Cluster-gcn: An efficient algorithm for training deep and large graph convolutional networks. In *Proceedings of the 25th ACM SIGKDD International Conference on Knowledge Discovery & Data Mining*, 257–266.
- [5] Edith Cohen and David D Lewis. 1999. Approximating matrix multiplication for pattern recognition tasks. *Journal of Algorithms* 30, 2 (1999), 211–252.
- [6] Weilin Cong, Rana Forsati, Mahmut Kandemir, and Mehrdad Mahdavi. 2020. Minimal variance sampling with provable guarantees for fast training of graph neural networks. In *Proceedings of the 26th ACM SIGKDD International Conference on Knowledge Discovery & Data Mining*, 1393–1403.
- [7] Tri Dao, Beidi Chen, Nimit S Sohoni, Arjun Desai, Michael Poli, Jessica Grogan, Alexander Liu, Aniruddh Rao, Atri Rudra, and Christopher Ré. 2022. Monarch: Expressive structured matrices for efficient and accurate training. In *International Conference on Machine Learning*. PMLR, 4690–4721.
- [8] Petros Drineas and Ravi Kannan. 2001. Fast Monte-Carlo algorithms for approximate matrix multiplication. In *Proceedings 42nd IEEE Symposium on Foundations of Computer Science*. IEEE, 452–459.
- [9] Petros Drineas, Ravi Kannan, and Michael W Mahoney. 2006. Fast Monte Carlo algorithms for matrices I: Approximating matrix multiplication. *SIAM J. Comput.* 36, 1 (2006), 132–157.
- [10] Petros Drineas, Ravi Kannan, and Michael W Mahoney. 2006. Fast Monte Carlo algorithms for matrices I: Approximating matrix multiplication. *SIAM J. Comput.* 36, 1 (2006), 132–157.
- [11] Keyu Duan, Zirui Liu, Peihao Wang, Wenqing Zheng, Kaixiong Zhou, Tianlong Chen, Xia Hu, and Zhangyang Wang. 2022. A Comprehensive Study on Large-Scale Graph Training: Benchmarking and Rethinking. (2022).
- [12] Keyu Duan, Zirui Liu, Peihao Wang, Wenqing Zheng, Kaixiong Zhou, Tianlong Chen, Xia Hu, and Zhangyang Wang. 2022. A Comprehensive Study on Large-Scale Graph Training: Benchmarking and Rethinking. In *Thirty-sixth Conference on Neural Information Processing Systems Datasets and Benchmarks Track*. https://openreview.net/forum?id=2QrFr_U782Z
- [13] Wenzheng Feng, Yuxiao Dong, Tinglin Huang, Ziqi Yin, Xu Cheng, Evgeny Kharlamov, and Jie Tang. 2022. GRAND+: Scalable Graph Random Neural Networks. In *Proceedings of the ACM Web Conference 2022*. 3248–3258.
- [14] Wenzheng Feng, Jie Zhang, Yuxiao Dong, Yu Han, Huanbo Luan, Qian Xu, Qiang Yang, Evgeny Kharlamov, and Jie Tang. 2020. Graph random neural networks for semi-supervised learning on graphs. *Advances in neural information processing systems* 33 (2020), 22092–22103.
- [15] Matthias Fey and Jan E. Lenssen. 2019. Fast Graph Representation Learning with PyTorch Geometric. In *ICLR Workshop on Representation Learning on Graphs and Manifolds*.
- [16] Xavier Glorot and Yoshua Bengio. 2010. Understanding the difficulty of training deep feedforward neural networks. In *Proceedings of the thirteenth international conference on artificial intelligence and statistics*. JMLR Workshop and Conference Proceedings, 249–256.
- [17] William L Hamilton, Rex Ying, and Jure Leskovec. 2017. Inductive representation learning on large graphs. In *Proceedings of the 31st International Conference on Neural Information Processing Systems*, 1025–1035.
- [18] Song Han, Xingyu Liu, Huizi Mao, Jing Pu, Ardavan Pedram, Mark A Horowitz, and William J Dally. 2016. EIE: Efficient inference engine on compressed deep neural network. *ACM SIGARCH Computer Architecture News* 44, 3 (2016), 243–254.
- [19] Song Han, Jeff Pool, John Tran, and William Dally. 2015. Learning both weights and connections for efficient neural network. *Advances in neural information processing systems* 28 (2015).
- [20] Xiaotian Han, Zhimeng Jiang, Ninghao Liu, and Xia Hu. 2022. G-Mixup: Graph Data Augmentation for Graph Classification. *arXiv preprint arXiv:2202.07179* (2022).
- [21] Weihua Hu, Matthias Fey, Marinka Zitnik, Yuxiao Dong, Hongyu Ren, Bowen Liu, Michele Catasta, and Jure Leskovec. 2020. Open graph benchmark: Datasets for machine learning on graphs. *arXiv preprint arXiv:2005.00687* (2020).
- [22] Guyue Huang, Guohao Dai, Yu Wang, and Huazhong Yang. 2020. Ge-spmv: General-purpose sparse matrix-matrix multiplication on gpus for graph neural networks. In *SC20: International Conference for High Performance Computing, Networking, Storage and Analysis*. IEEE, 1–12.
- [23] Wenbing Huang, Tong Zhang, Yu Rong, and Junzhou Huang. 2018. Adaptive sampling towards fast graph representation learning. In *Advances in Neural Information Processing Systems*.
- [24] Zhimeng Jiang, Xiaotian Han, Chao Fan, Zirui Liu, Na Zou, Ali Mostafavi, and Xia Hu. 2022. Fmp: Toward fair graph message passing against topology bias. *arXiv preprint arXiv:2202.04187* (2022).
- [25] Thomas N Kipf and Max Welling. 2017. Semi-supervised classification with graph convolutional networks. In *International Conference on Learning Representations*. <https://openreview.net/forum?id=SJU4ayYgl>
- [26] Yuanzhi Li, Colin Wei, and Tengyu Ma. 2019. Towards explaining the regularization effect of initial large learning rate in training neural networks. *Advances in Neural Information Processing Systems* 32 (2019).
- [27] Zirui Liu, Haifeng Jin, Ting-Hsiang Wang, Kaixiong Zhou, and Xia Hu. 2021. DivAug: Plug-in Automated Data Augmentation with Explicit Diversity Maximization. In *Proceedings of the IEEE/CVF International Conference on Computer Vision*. 4762–4770.
- [28] Zirui Liu, Kaixiong Zhou, Fan Yang, Li Li, Rui Chen, and Xia Hu. 2022. EXACT: Scalable Graph Neural Networks Training via Extreme Activation Compression. In *International Conference on Learning Representations*. https://openreview.net/forum?id=vkaMaq95_rX
- [29] S Deepak Narayanan, Aditya Sinha, Prateek Jain, Purushottam Kar, and SUN-DARAJAN SELLAMANICKAM. 2022. IGLU: Efficient GCN Training via Lazy Updates. In *International Conference on Learning Representations*. <https://openreview.net/forum?id=5kq11T11z4>
- [30] Md Khaledur Rahman, Majedul Haque Sujon, and Ariful Azad. 2021. Fusedmm: A unified sddmm-spmv kernel for graph embedding and graph neural networks. In *2021 IEEE International Parallel and Distributed Processing Symposium (IPDPS)*. IEEE, 256–266.
- [31] Morteza Ramezani, Weilin Cong, Mehrdad Mahdavi, Mahmut Kandemir, and Anand Sivasubramanian. 2022. Learn Locally, Correct Globally: A Distributed Algorithm for Training Graph Neural Networks. In *International Conference on Learning Representations*. <https://openreview.net/forum?id=FndDxSz3LxQ>
- [32] Yu Rong, Wenbing Huang, Tingyang Xu, and Junzhou Huang. 2019. Dropedge: Towards deep graph convolutional networks on node classification. *arXiv preprint arXiv:1907.10903* (2019).
- [33] Petar Veličković, Guillem Cucurull, Arantxa Casanova, Adriana Romero, Pietro Lio, and Yoshua Bengio. 2017. Graph attention networks. In *International Conference on Learning Representations*.
- [34] Cheng Wan, Youjie Li, Cameron R Wolfe, Anastasios Kyrillidis, Nam Sung Kim, and Yingyan Lin. 2022. Pipegcn: Efficient full-graph training of graph convolutional networks with pipelined feature communication. *arXiv preprint arXiv:2203.10428* (2022).
- [35] Minjie Wang, Da Zheng, Zihao Ye, Quan Gan, Mufei Li, Xiang Song, Jinjing Zhou, Chao Ma, Lingfan Yu, Yu Gai, Tianjun Xiao, Tong He, George Karypis, Jinyang Li, and Zheng Zhang. 2019. Deep Graph Library: A Graph-Centric, Highly-Performant Package for Graph Neural Networks. *arXiv preprint arXiv:1909.01315* (2019).

- [36] Rex Ying, Ruining He, Kaifeng Chen, Pong Eksombatchai, William L Hamilton, and Jure Leskovec. 2018. Graph convolutional neural networks for web-scale recommender systems. In *Proceedings of the 24th ACM SIGKDD International Conference on Knowledge Discovery & Data Mining*. 974–983.
- [37] Yang You, Jing Li, Sashank Reddi, Jonathan Hseu, Sanjiv Kumar, Srinadh Bhojanapalli, Xiaodan Song, James Demmel, Kurt Keutzer, and Cho-Jui Hsieh. 2019. Large batch optimization for deep learning: Training bert in 76 minutes. *arXiv preprint arXiv:1904.00962* (2019).
- [38] Hanqing Zeng, Hongkuan Zhou, Ajitesh Srivastava, Rajgopal Kannan, and Viktor Prasanna. 2020. GraphSAINT: Graph Sampling Based Inductive Learning Method. In *International Conference on Learning Representations*. <https://openreview.net/forum?id=BJe8pkHFwS>
- [39] Hengrui Zhang, Zhongming Yu, Guohao Dai, Guyue Huang, Yufei Ding, Yuan Xie, and Yu Wang. 2022. Understanding gnn computational graph: A coordinated computation, io, and memory perspective. *Proceedings of Machine Learning and Systems* 4 (2022), 467–484.
- [40] Da Zheng, Chao Ma, Minjie Wang, Jinjing Zhou, Qidong Su, Xiang Song, Quan Gan, Zheng Zhang, and George Karypis. 2020. Distgl: distributed graph neural network training for billion-scale graphs. In *2020 IEEE/ACM 10th Workshop on Irregular Applications: Architectures and Algorithms (IA3)*. IEEE, 36–44.
- [41] Difan Zou, Ziniu Hu, Yewen Wang, Song Jiang, Yizhou Sun, and Ququan Gu. 2019. Layer-dependent importance sampling for training deep and large graph convolutional networks. *arXiv preprint arXiv:1911.07323* (2019).

A MATHEMATICAL ANALYSIS

A.1 Proof of Proposition 1

Proposition 1 (Proof in Appendix A). *If the approximation method is itself unbiased, and we only replace the SpMM in the backward pass with its approximated version, while leaving the forward one unchanged, then the calculated gradient is provably unbiased.*

Here we note that in the main text, for the notation convenience, we ignore the backward pass of ReLU. However, the proof here will consider the non-linear activation function to prove the unbiasedness. Let $H_{pre}^{(l+1)} = \text{SpMM}(\tilde{A}, J^{(l)})$ be the pre-activation. The backward pass of ReLU is:

$$\begin{aligned} \mathbb{E}[\nabla H_{pre}^{(l+1)}] &= \mathbb{E}[\mathbb{1}_{H_{pre}^{(l+1)} > 0} \odot \nabla H^{(l+1)}] \\ &= \mathbb{1}_{H_{pre}^{(l+1)} > 0} \odot \mathbb{E}[\nabla H^{(l+1)}], \end{aligned} \quad (6)$$

where \odot is the element-wise product and $\mathbb{1}$ is the indicator function. The element-wise product is linear operation and $\mathbb{1}_{H_{pre}^{(l+1)} > 0}$ is only related to the pre-activation in the forward pass, we only apply the approximation during the backward pass so $\mathbb{1}_{H_{pre}^{(l+1)} > 0}$ can be extracted from the expectation. We know that for the last layer, we have $\mathbb{E}[\nabla H^{(L)}] = H^{(L)}$ since we do not apply ReLU at the output layer. We then can prove by induction that $\mathbb{E}[\nabla H^{(l+1)}] = H^{(l+1)}$ and $\mathbb{E}[\nabla J^{(l)}] = \mathbb{E}[\text{approx}(\tilde{A}^\top \nabla H_{pre}^{(l+1)})] = \nabla J^{(l)}$ for any layer l .

A.2 Analysis of MEAN aggregator

For GraphSAGE, one commonly used aggregator is the MEAN aggregator, which can be expressed as follows:

$$H^{(l+1)} = W_1 H^{(l)} + W_2 \text{SpMM_MEAN}(A, H^{(l)}), \quad (7)$$

where SpMM_MEAN is one variant of the vanilla SpMM, which replace the reducer function from $\text{sum}(\cdot)$ to $\text{mean}(\cdot)$. We note that in popular GNN packages, the MEAN aggregator usually is implemented based on SpMM_MEAN [15, 35] to reduce the memory usage. Here we give an example of SpMM_MEAN to illustrate how it works:

$$\text{SpMM_MEAN}\left(\begin{bmatrix} 1 & 0 \\ 0 & 4 \\ 5 & 6 \end{bmatrix}, \begin{bmatrix} 7 & 8 \\ 9 & 10 \end{bmatrix}\right) = \begin{bmatrix} \frac{1}{2}(1 \times 7 + 0 \times 9) & \frac{1}{2}(1 \times 8 + 0 \times 10) \\ \frac{1}{4}(0 \times 7 + 4 \times 9) & \frac{1}{4}(0 \times 8 + 4 \times 10) \\ \frac{1}{2}(5 \times 7 + 6 \times 9) & \frac{1}{2}(5 \times 8 + 6 \times 10) \end{bmatrix},$$

Equivalently, the SpMM_MEAN can also be expressed as:

$$\text{SpMM_MEAN}(A, H^{(l)}) = D^{-1} A H^{(l)},$$

where D is the degree matrix of A . Thus, although we did not normalize the adjacency matrix in GraphSAGE, when applying the top- k sampling to approximate SpMM_MEAN, the column norm of $A_{:,j_i}$ is actually $\frac{1}{\sqrt{\text{Deg}_{j_i}}}$ due to the normalization.

Also, for GraphSAGE, the inputs to the first SpMM_MEAN operation are A and X . They do not require gradient since they are not trainable. Thus, the first SAGE layer is not presented in Figure 9 and Figure 7.

B PSEUDO CODE OF THE GREEDY ALGORITHM

In algorithm 1, here we provide the pseudo code of our greedy algorithm for solving the constrained optimization problem. In Table 5, we show the run time of the greedy algorithm, which is negligible compared to the acceleration effect.

Table 5: The running time (second) of the greedy algorithm.

	Reddit	Yelp	ogbn-proteins	ogbn-products
GCN	0.03	0.03	0.03	0.03
GraphSAGE	0.02	0.02	0.03	0.03
GCNII	0.05	0.05	0.06	-

C EXPERIMENTAL SETTINGS

C.1 Software and Hardware Descriptions

All experiments are conducted on a server with four NVIDIA 3090 GPUs, four AMD EPYC 7282 CPUs, and 252GB host memory. We implement all models based on Pytorch and Pytorch Geometric. During our experiments, we found that the version of Pytorch, Pytorch Sparse, and Pytorch Scatter can significantly impact the running speed of the baseline. Here we list the details of our used packages in all experiments in Table 6.

Table 6: Package configurations of our experiments.

Package	Version
CUDA	11.1
pytorch_sparse	0.6.12
pytorch_scatter	2.0.8
pytorch_geometric	1.7.2
pytorch	1.9.0
OGB	1.3.2

C.2 Statistics of benchmark datasets

The statistics for all used datasets are shown in Table 7. We follow the standard data splits and all datasets are directly downloaded from Pytorch Geometric or the protocol of OGB [21].

Algorithm 1: The greedy algorithm

Input: The gradients of node embeddings $\{\nabla H^{(1)}, \dots, \nabla H^{(L)}\}$, the adjacency matrix A , the hidden dimension $\{d_1, \dots, d_L\}$, the node set \mathcal{V} , the edge set \mathcal{E}

Parameters: The step size α , the overall budget C

Output: The layer-wise $\{k_1, \dots, k_L\}$ associated with the top- k sampling

```

1  $B \leftarrow \sum_{l=1}^L |\mathcal{E}| d_l$ 
2  $\forall i, k_l \leftarrow |\mathcal{V}|, \text{Top}_{k_l} \leftarrow \{1, \dots, |\mathcal{V}|\}$ .
3 while  $B \geq C \sum_{l=1}^L |\mathcal{E}| d_l$  do
4    $m \leftarrow \arg \min_{l \in \{1, \dots, L\}} (\sum_{i \in \text{Top}_{k_l}} \|A_{:,i}^\top\|_2 \|\nabla H_{i,:}^{(l+1)}\|_2 - \sum_{i \in \text{Top}_{k_l - \alpha|\mathcal{V}|}} \|A_{:,i}^\top\|_2 \|\nabla H_{i,:}^{(l+1)}\|_2)$ 
   // Choose the layer  $m$  to reduce by a step size  $\alpha|\mathcal{V}|$ , such that the increment of errors is minimal.
5    $B \leftarrow B - d_m \sum_{i \in \text{Top}_{k_m} \cap i \notin \text{Top}_{k_m - \alpha|\mathcal{V}|}} \#nnz_i$ 
   // Since we exclude some column-row pairs for layer  $m$ , here we reduce the budget  $B$  accordingly.
6    $k_m \leftarrow k_m - \alpha|\mathcal{V}|$ 
   // Update  $k_m$  accordingly.
7    $\text{Top}_{k_m} \leftarrow$  the set of indices  $i$  associated with  $k_m$  largest  $\|A_{:,i}^\top\|_2 \|\nabla H_{i,:}^{(l+1)}\|_2$ 
   // Update  $\text{Top}_{k_m}$  accordingly.
8 end
9 return  $\{k_1, \dots, k_L\}$ 

```

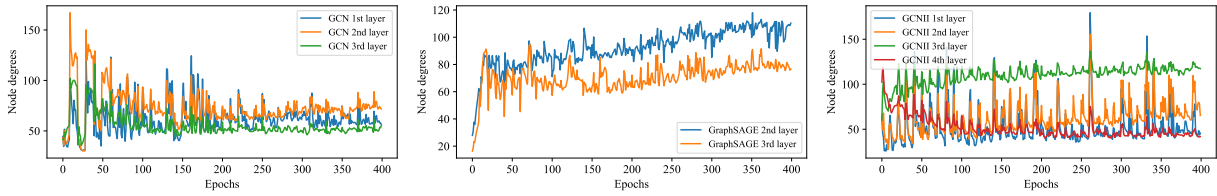


Figure 9: The averaged degrees of nodes picked by top- k sampling along the whole training process, where the applied dataset is Reddit and overall budget C is set as 0.1.

Table 8: Configuration of Full-Batch GCN.

Dataset	Training			Architecture		
	Learning Rates	Epochs	Dropout	BatchNorm	Layers	Hidden Dimension
Reddit	0.01	400	0.5	Yes	3	256
Yelp	0.01	500	0.1	Yes	3	512
ogbn-proteins	0.01	1000	0.5	No	3	256
ogbn-products	0.001	500	0.5	No	3	256

Table 9: Configuration of Full-Batch GraphSAGE.

Dataset	Training			Architecture		
	Learning Rates	Epochs	Dropout	BatchNorm	Layers	Hidden Dimension
Reddit	0.01	400	0.5	Yes	3	256
Yelp	0.01	500	0.1	Yes	3	512
ogbn-proteins	0.01	1000	0.5	No	3	256
ogbn-products	0.001	500	0.5	No	3	256

Table 10: Configuration of Full-Batch GCNII.

Dataset	Training			Architecture		
	Learning Rates	Epochs	Dropout	BatchNorm	Layers	Hidden Dimension
Reddit	0.01	400	0.5	Yes	4	256
Yelp	0.01	500	0.1	Yes	4	256
ogbn-proteins	0.01	1000	0.5	No	4	256

Table 11: Training configuration of GraphSAINT.

Dataset	RandomWalk Sampler		Training			Architecture		
	Walk length	Roots	Learning Rates	Epochs	Dropout	BatchNorm	Layers	Hidden Dimension
Reddit	4	8000	0.01	40	0.1	Yes	3	128
Yelp	2	8000	0.01	75	0.1	Yes	3	512
ogbn-products	3	60000	0.01	20	0.5	No	3	256

Table 7: Dataset Statistics.

Dataset	Task	Nodes	Edges	Classes	Label Rates
Reddit	multi-class	232,965	11,606,919	41	65.86%
Yelp	multi-label	716,847	6,977,409	100	75.00%
ogbn-proteins	binary-Class	132,534	39,561,252	2	65.00%
ogbn-products	multi-class	2,449,029	61,859,076	47	8.03%

C.3 Hyperparameter Settings

Regarding Reddit, and Yelp dataset, we follow the hyperparameter configurations reported in the respective papers as closely as possible. Regarding *ogbn-proteins* and *ogbn-products* dataset, we follow the hyperparameter configurations and codebases provided on the OGB [21] leader-board. Please refer to the OGB website for more details. The optimizer is Adam for all these models. All methods terminate after a fixed number of epochs. We report the test accuracy associated with the highest validation score. Table 11 summarize the hyperparameter configuration of GraphSAINT.

Table 8, Table 9, and Table 10 summarize the hyperparameter configuration of full-Batch GCN, full-Batch GraphSAGE, and full-batch GCNII, respectively.